Phase coherence is not related to topology

Leandro Freitas [*]
Instituto Federal de Educação, Ciência e Tecnologia de Minas Gerais, Campus Betim Rua Itaguaçu 595, 32.677-562 Betim, MG, Brazil

Leonardo L. Portes,[†] Leonardo A. B. Torres,[‡] and Luis A. Aguirre[§]
Programa de Pós-Graduação em Engenharia Elétrica, Universidade Federal de Minas Gerais, Avenida Antônio Carlos 6627, 31270-901 Belo Horizonte, MG, Brazil

(Received 20 June 2018; revised manuscript received 4 November 2019; accepted 16 January 2020; published 12 March 2020)

Phase coherence is an important measure in nonlinear science. Whereas there is no generally accepted definition for phase and therefore for phase coherence, many works associate this feature with topological aspects of the systems, such as having a well-defined rotating center. Given the relevance of this concept for synchronization problems, one aim of this paper is to argue by means of a couple of counterexamples that phase coherence is not related to the topology of the attractor. A second aim is to introduce a phase-coherence measure based on recurrence plots, for which probabilities of recurrences for two different trajectories are similar for a phase-coherent system and dissimilar for non-phase-coherent systems. The measure does not require a phase variable defined *a priori*.

DOI: 10.1103/PhysRevE.101.032207

I. INTRODUCTION

The study of chaotic phase synchronization (PS) [1] has received considerable attention in recent years and contributed to understand many natural phenomena in different fields (e.g., [2–4]). Unfortunately, a general characterization of such phenomena is still lacking, mostly due to the wide variety of attractors, with great diversity of topologies and dynamics, for which it is hard even to define a proper *phase variable* in a general way [5]. Hence, different and very often nonequivalent metrics have been used in the study of PS, which are associated with timescales, phase coherence, attractor topology, etc., in cases for which custom phase definitions have been proposed.

A phase variable has spatial and rhythmic properties [6], where the former refers to recurrence features in the state space and the latter refers to the elapsed time between these recurrences. These two distinct characteristics can clarify the role of some concepts in nonlinear dynamics. Whereas there is no generally accepted definition for phase coherence, many works refer to it as a spatial feature, related to the easiness of finding a proper rotating center, e.g., [7–13]. In several works, topological attributes of the attractor, such as *funnel* or *screw type*, are related to the lack of *phase coherence*. Perhaps, this is motivated by the largely used benchmark Rössler oscillator, where the non-phase-coherence emerges together with a funnel topology.

The present paper contests this point of view and shows that the phase coherence is essentially a rhythmic property of the oscillator, which is not related to the topology of the attractor. Counterexamples of a phase-coherent-funnel and a non-phase-coherent-spiral oscillator are provided using standard measures of phase coherence. In addition, a measure based on recurrence plots is introduced, which provides statistically significant results in distinguishing phase coherence, without requiring a phase variable.

This paper is organized as follows. Section II provides background material. A key tool used in the paper is time reparametrization of ordinary differential equations; this is quickly reviewed in Sec. III and illustrated in Sec. IV. The proposed measure of phase coherence is presented in Sec. V. The main conclusions are presented in Sec. VI.

II. BACKGROUND

The concept of phase coherence has different interpretations in the scientific literature. The term was used by Farmer and coworkers in the spectral analysis of chaotic attractors [14,15]. It was stated that phase-coherent systems "have power spectra that are superpositions of delta functions and broad backgrounds" [14] and it was argued that the system could be decomposed into periodic and nonperiodic subsystems, where the first is responsible for the peaks and the latter is responsible for for the broad background in the spectrum. Later, Stone [16] introduced the term in the context of frequency entrainment of chaotic oscillators.

Some more recent works have linked the concepts of phase coherence with topological aspects of the attractor, e.g., the ease to find a proper rotating center [7–13]. However, no clear connection between such concepts seems to exist, as shown in the sequel.

[*]leandro.freitas@ifmg.edu.br
[†]Present address: Complex Systems Group, Department of Mathematics and Statistics, University of Western Australia, Nedlands, Perth, WA 6009, Australia; ll.portes@gmail.com
[‡]leotorres@ufmg.br
[§]aguirre@ufmg.br

In this paper, the terms *topology*, *spatial features*, and *geometry* refer to features of a chaotic attractor as an object: a set of trajectories organized in a particular shape. This terminology is inspired by the topological analysis, that investigates the stretching and squeezing mechanisms that act to create a strange attractor and organize all the unstable periodic orbits in the attractor [17–19] in terms of branched manifolds, bounding tori, genus, etc. In these analyses, the *rhythm* of the evolution is not essential. In the context of this paper, geometry or topological aspects refer to characteristics of the shape of the attractor in the state space.

One of the most used measures of phase coherence is the phase diffusion coefficient, which is based on a statistical analysis of the behavior of a phase variable, in terms of a stochastic diffusion model [20]. It considers that the time derivative of a phase variable (frequency) can be approximated by a constant term ω (mean frequency) added to a random noise $\xi(t)$, leading to $\phi(t) = \phi_0 + \omega t + \int_0^t \xi(\tau) d\tau$. The fluctuation strength of $\phi(t)$ can be evaluated by the variance

$$\sigma^2(t) \equiv \langle [\phi(t) - \phi_0 - \omega t]^2 \rangle \propto 2Dt, \tag{1}$$

where $\langle \cdot \rangle$ denotes the ensemble average and D denotes the phase diffusion coefficient.

A coherent oscillation occurs when $D \approx 0$. However, for chaotic oscillators, it is worth pointing out that this coefficient requires a phase variable defined *a priori*, which carries many unclear issues related to the problem of defining such a phase [5].

Some works use the coherence factor [21,22], that does not require an explicit phase variable and is calculated with the help of a Poincaré section $\mathcal{P}$ as

$$\chi_{\mathrm{CF}}^{(\mathcal{P})} = \frac{\langle T^{(\mathcal{P})} \rangle}{\sigma_T^{(\mathcal{P})}}, \tag{2}$$

where T denotes the time between consecutive crossings of the Poincaré section and σ_T, its standard deviation.

The main drawback lies in the choice of a proper Poincaré section. The coherence factor χ_{CF} seems to be useful for comparing very similar systems (e.g., with and without some addition of noise) [23], but it can be meaningless for comparing very different systems. Perhaps some optimal Poincaré section (see, e.g., [24]) should be used for such a purpose.

A measure that does not require either a phase variable or a Poincaré section has been proposed [12]. It is based on recurrence properties of the system [25], described by the recurrence matrix

$$R_{i,j}^{(\epsilon)} = \Theta(\epsilon - \|\boldsymbol{x}_i - \boldsymbol{x}_j\|), \tag{3}$$

where $\Theta(\cdot)$ is the Heaviside function, $\epsilon \in \mathbb{R}$ is a predefined threshold, $\boldsymbol{x} \in \mathbb{R}^n$ is the state vector, and i and j are discrete-time indices.

A notion of the rhythm of the system is quantified by the recurrence time τ (given in samples), which is the time between recurrent points. The probability of recurrence at τ can be obtained directly from the recurrence matrix (3) as

$$P^{(\epsilon)}(\tau) = \frac{\sum_{i=1}^{N-\tau} R_{i,i+\tau}^{(\epsilon)}}{N - \tau}, \tag{4}$$

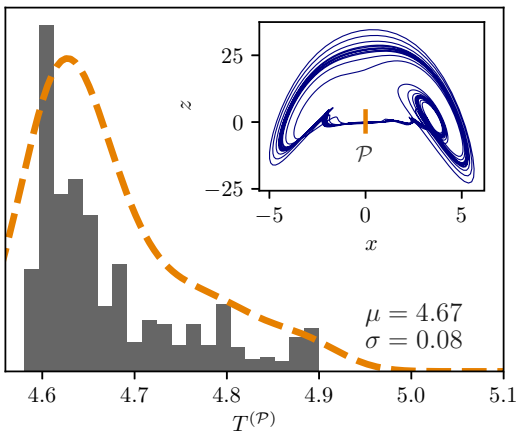

FIG. 1. Histogram of returning times to the Poincaré section $\mathcal{P} = \{\boldsymbol{x} : x = 0,\ \dot{x} > 0\}$ for the chaotic Cord system [27] with parameters $(a,\ b,\ F,\ G) = (0.258,\ 4.033,\ 8.0,\ 1.0)$. A smooth density function (orange dashed line) was fitted to guide the eye. The embedded figure shows the (x, z) projection of the attractor with the corresponding Poincaré section.

where N is the data length. The $P^{(\epsilon)}(\tau)$ is also known as the generalized autocorrelation function and has been used to quantify phase synchronization between oscillators 1 and 2 by means of the correlation coefficient [26]:

$$\rho_{\mathrm{CPR}}^{(\epsilon)} = \frac{\langle \bar{P}_1^{(\epsilon)}(\tau)\, \bar{P}_2^{(\epsilon)}(\tau) \rangle}{\sigma_1^{(\epsilon)}\, \sigma_2^{(\epsilon)}}, \tag{5}$$

where $\langle \cdot \rangle$ indicate time averaging over τ, and for the ith oscillator the $\bar{P}_i^{(\epsilon)}$ means that the average has been subtracted and σ_i is the respective standard deviation. A $\rho_{\mathrm{CPR}} \approx 1$ indicates phase synchronization.

To quantify the phase coherence, the so-called generalized coherence factor has been proposed [12]:

$$\chi_{\mathrm{GCF}}^{(\epsilon)} = \frac{\langle \tau \rangle^{(\epsilon)}}{\sigma_\tau^{(\epsilon)}}, \tag{6}$$

where $\langle \tau \rangle^{(\epsilon)}$ and $\sigma_\tau^{(\epsilon)}$ are the mean and standard deviation of recurrent times taken from (4). This index, however, did not achieve a high level of significance in distinguishing noncoherent from coherent dynamics for the Rössler system [12].

Note that the phase diffusion coefficient (1), the returning times to a Poincaré section (2), and the generalized coherence factor (6) relate to rhythmic characteristics of the system. Other commonly mentioned features, such as the ease to find a proper rotating center [7–13], or if the phase of some Hilbert-transformed observable increases monotonically [12,13], relate to topological characteristics of the oscillator.

These two points of view are not related in general. An interesting example is provided by the Cord attractor [27], which in spite of having a very regular returning time (i.e., low variance) with small phase diffusion ($D = 0.05$) has a challenging topology [28] without a single rotating center, as shown in Fig. 1.

III. TIME REPARAMETRIZATION

To argue in favor of the lack of relation between topology and phase coherence, consider a nonlinear oscillator described by

$$\dot{\boldsymbol{x}} = \boldsymbol{f}(\boldsymbol{x}), \tag{7}$$

where the $\boldsymbol{x} \in \mathbb{R}^n$ is the state vector, $\boldsymbol{f} : \mathbb{R}^n \to \mathbb{R}^n$ is a nonlinear vector function, and, for some initial condition $\boldsymbol{x}_0 \equiv \boldsymbol{x}(0)$—which is not an equilibrium point, i.e., $\boldsymbol{f}(\boldsymbol{x}_0) \neq \boldsymbol{0}$—the solution of (7) exists, it is unique, and its trajectories converge to an attractor $\Gamma \subset \mathbb{R}^n$.

Now we introduce a modified version of (7):

$$\dot{\boldsymbol{x}} = r(\boldsymbol{x})\,\boldsymbol{f}(\boldsymbol{x}), \tag{8}$$

where $r : \mathbb{R}^n \to \mathbb{R}^+$ is a positive smooth scalar function.

The introduction of $r(\boldsymbol{x})$ is a well-known method in the analysis of ordinary differential equations and it leads to a reparametrization of time [29], where the flow and the attractor Γ remain at exactly the same spatial location for both systems (7) and (8), but the time evolution can be stretched or shrunk at each point of $\mathbb{R}^n$, according to $r(\boldsymbol{x})$. It provides an interesting tool for analysis because it surgically isolates the two aforementioned elements: on the one hand the *rhythm*, related to $r(\boldsymbol{x})$; and, on the other, the *spatial* (or topological) characteristic, related to $\boldsymbol{f}(\boldsymbol{x})$.

Note that this procedure can be applied to any system described as (7). It shows that the rhythm can be changed independently of the geometry of the attractor. Despite the general applicability of this procedure, on oscillators of any dimension, in what follows, this property will be used to modify some specific benchmark systems in order to confirm that, in fact, topology does not have any *general* relation to phase coherence.

IV. COHERENT FUNNEL AND NONCOHERENT SPIRAL

The Rössler system is given by (7) with

$$\boldsymbol{f}(\boldsymbol{x}) = \begin{bmatrix} -y - z \\ x + ay \\ b + z(x - c) \end{bmatrix}, \tag{9}$$

where $\boldsymbol{x} \equiv [x,\ y,\ z]^\top$, $(b, c) = (0.1, 8.5)$, and the parameter a is used to switch between spiral ($a = 0.16$) and funnel ($a = 0.3$) behaviors. A proper Poincaré section can be defined regardless of the dynamic behavior [17] as

$$\mathcal{P}_r = \left\{ (y, z) \in \mathbb{R}^2 : x = \frac{c - \sqrt{c^2 - 4ab}}{2},\ \dot{x} > 0 \right\}. \tag{10}$$

We introduce the *non-phase-coherent*-spiral oscillator by modifying the Rössler system, described as (8) with (9); parameter $a = 0.16$ (spiral); and the *ad hoc* choice:

$$r(\boldsymbol{x}) := 0.01 + 0.05(x^2 + y^2), \tag{11}$$

where $r(\boldsymbol{x}) > 0, \forall \boldsymbol{x} \in \mathbb{R}^n$.

The *phase-coherent*-funnel oscillator is introduced similarly, by using $a = 0.3$ (funnel) and taking

$$r(\boldsymbol{x}) := 0.546 - 0.471 \tanh\left(\frac{z - 25.5}{11}\right), \tag{12}$$

where as before $r(\boldsymbol{x}) > 0, \forall \boldsymbol{x} \in \mathbb{R}^n$.

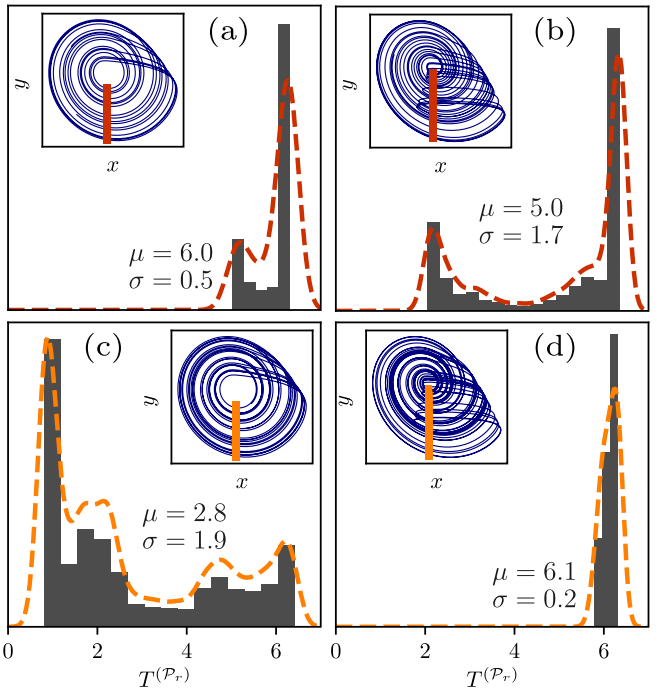

FIG. 2. Histograms of returning times of the (a) spiral Rössler, (b) funnel Rössler, (c) *non-phase-coherent*-spiral system with (11), and (d) *phase-coherent*-funnel system that uses (12), with respect to the Poincaré section $\mathcal{P}_r$ (10). For each histogram, a smooth density function (dashed line) was fitted to guide the eye. The embedded figures show the $(x,\ y)$ projection of the corresponding attractor and Poincaré section.

Clearly, as shown in Fig. 2, the returning time for the *non-phase-coherent*-spiral [Fig. 2(c)] system has the highest dispersion corresponding to a very irregular dynamic (rhythmic) evolution. On the other hand, the returning times for the *phase-coherent*-funnel [Fig. 2(d)] system are restricted to a narrow range, and indicate time regularity even greater than for the classical spiral attractor [Fig. 2(b)].

This analysis can be readily confirmed by the power spectrum density of each state variable (Fig. 3). Comparing the

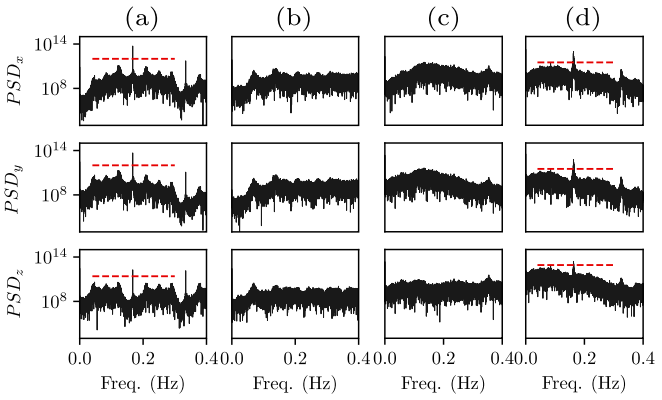

FIG. 3. Power spectrum density of the (a) spiral Rössler, (b) *non-phase-coherent*-spiral system, (c) funnel Rössler, and (d) *phase-coherent*-funnel system, for each variable, respectively, from top to bottom: x, y, and z. A straight dashed red line was added to detect the peaks.

original spiral and funnel Rössler oscillators [Figs. 3(a) and 3(c)], it is straightforward to distinguish between the phase-coherent and noncoherent behaviors, where the existence of a clear peak with a broad background [Fig. 3(a)] is the signature of phase coherence [14]. This signature can also be observed for the *phase-coherent*-funnel [Fig. 3(d)], but not for the *non-phase-coherent*-spiral [Fig. 3(b)], system. The phase diffusion index (1) corroborates with the analysis, where $D = 0.009$ for the spiral and $D = 0.332$ for the funnel Rössler; $D = 2.661$ for the *non-phase-coherent*-spiral and $D = 0.005$ for the *phase-coherent*-funnel systems.

The notion of phase coherence should not be associated to topological aspects of the attractor. Hence, it seems that to relate coherence and the ease with which a phase variable can be defined as a scalar function of the states is not generally true. Following the same line of reasoning, it is conjectured that many rotating centers do not necessarily imply many timescales and vice versa.

V. COHERENCE AND RECURRENCE

Topological properties of an attractor have no bearing on phase coherence, and the probability of recurrence (4) can be used instead. This probability function displays regular peaks in the presence of phase coherence and irregular patterns indicate a noncoherent phase [26]. Figures 4(a)–4(d) show those different patterns, where the rhythm of recurrence (lag τ) seems to be roughly predictable for phase-coherent systems.

Returning times were used in quantifying phase coherence by Zou *et al.* [12]. In that work, index χ_{GCF} (6) was proposed, although it was unable to clearly detect phase coherence in a benchmark problem with Rössler oscillators. A different approach is proposed next.

Phase-coherent systems possess trajectories that recur at very regular time lags. Each subplot in Fig. 4 shows the probability of recurrence (4) computed for two distinct trajectories of the same system, denoted in different colors. The two trajectories were simulated from different initial conditions from the same oscillator.

Based on such a procedure, a very simple yet effective principle is proposed here as a way for detecting phase coherence; namely, two probabilities [see Eq. (4)] of recurrences will be very similar only for a phase-coherent system, as illustrated in Fig. 4.

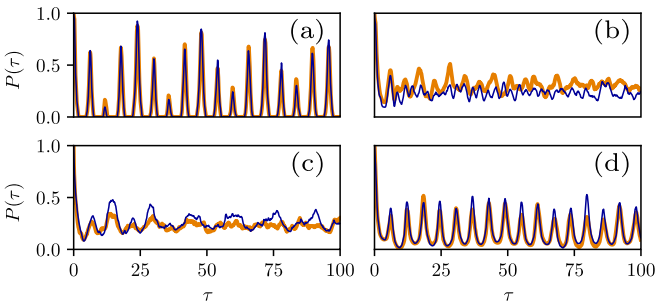

FIG. 4. Probabilities of recurrence for the (a) spiral and (b) funnel Rössler and (c) noncoherent-spiral and (d) coherent-funnel systems. The threshold ϵ was chosen in order to achieve about 6% recurrence rate. The different colors denote different realizations using the same system.

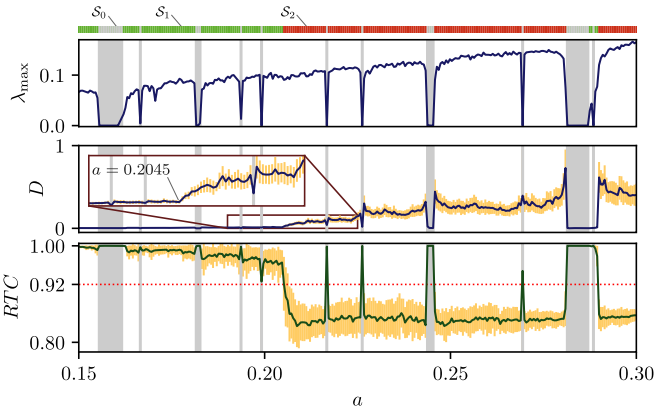

FIG. 5. From top: Maximum Lyapunov exponent, phase diffusion coefficient, and RTC index (χ_{RTC}) for the Rössler oscillator (9) with $(b, c) = (0.4, 8.5)$. The average (solid line) and standard deviation (yellow bars) of D and RTC were taken from 100 Monte Carlo runs. The gray areas correspond to periodic windows ($\lambda_{\max} < 0.02$). The sets $\mathcal{S}_0$, $\mathcal{S}_1$, and $\mathcal{S}_2$ are identified by the colorbar on the very top.

More formally, for a system described as (7), consider two different finite trajectories $\gamma_a(t; x_{0,a})$ and $\gamma_b(t; x_{0,b})$, with different initial conditions $x_{0,a}, x_{0,b} \in \Gamma$, taken from the same system (7). The probability of recurrence (4) is computed over each trajectory, denoted, respectively, by $P^{(\epsilon,\gamma_a)}(\tau)$ and $P^{(\epsilon,\gamma_b)}(\tau)$. The proposed recurrence time coherence (RTC) is computed as

$$\chi_{\mathrm{RTC}}^{(\epsilon,\gamma_a,\gamma_b)} = \frac{\langle \bar{P}^{(\epsilon,\gamma_a)}(\tau)\, \bar{P}^{(\epsilon,\gamma_b)}(\tau)\rangle}{\sigma^{(\epsilon,\gamma_a)}\, \sigma^{(\epsilon,\gamma_b)}}, \tag{13}$$

where $\bar{P}^{(\epsilon,\gamma_i)}(\tau)$ is the probability computed using the ith trajectory of the system. Note that the computation of (13) is very similar to (5). In the case of (13), $\bar{P}$ is computed for two trajectories *of the same system*, whereas in (5) it is computed for two different systems.

The basic idea is that phase-coherent systems have high probability of recurrence at regular time lags τ, whereas non-phase-coherent systems yield irregular patterns of $\bar{P}^{(\epsilon,\gamma_i)}(\tau)$ for each ith realization (Fig. 4). A high value, $\chi_{\mathrm{RTC}} \approx 1$, corresponds to phase-coherent dynamics.

In order to systematically evaluate the performance of the χ_{RTC} index in distinguishing noncoherent and phase-coherent behaviors, following [12], the Wilcoxon-Mann-Whitney U test is performed for the Rössler system (9) with $(b, c) = (0.4, 8.5)$ and 300 equally spaced values in the interval $a \in [0.15, 0.3]$. For each a, the maximum Lyapunov exponent ($\lambda_{\max}$), 100 Monte Carlo runs of the phase diffusion coefficient (D), and the RTC index (χ_{RTC}) were computed. Those values are shown in Fig. 5, where it is possible to clearly identify the onset of the noncoherent behavior. Three sets of behaviors were identified as periodic ($\mathcal{S}_0$), phase coherent ($\mathcal{S}_1$), and non-phase-coherent ($\mathcal{S}_2$):

$$\mathcal{S}_0 = \{\chi_{\mathrm{RTC}}(a) : \lambda_{\max}(a) < 0.02\},$$
$$\mathcal{S}_1 = \{\chi_{\mathrm{RTC}}(a) : \lambda_{\max}(a) \geqslant 0.02 \cap \bar{D}(a) < 0.02\},$$
$$\mathcal{S}_2 = \{\chi_{\mathrm{RTC}}(a) : \lambda_{\max}(a) \geqslant 0.02 \cap \bar{D}(a) \geqslant 0.02\},$$

where $\bar{D}$ denotes the average of D over the 100 Monte Carlo runs.

The statistical test revealed that the RTC index can distinguish between coherent ($\mathcal{S}_1$) and noncoherent ($\mathcal{S}_2$) behaviors with high level of significance [30]. The average and standard deviations of the phase-coherent behavior are $\mu_1 = 0.98$ and $\sigma_1 = 0.02$, and for the noncoherent behavior they are $\mu_2 = 0.85$ and $\sigma_2 = 0.03$. As a rule of thumb, if one considers a noncoherent behavior for $\chi_{\mathrm{RTC}} < 0.92$, a successful rate of 98.6% in the classification is observed in the analyzed case (red dotted line in Fig. 5).

The RTC index was also applied to other chaotic systems with nontrivial topology such as the Cord [27] and Li [31] oscillators. The results attained similar performance as the phase diffusion coefficient. One of the main advantages of the RTC index is that it does not require a phase variable defined *a priori*.

VI. CONCLUSIONS

The concept of phase coherence should not be associated with topological features of the attractor. A procedure with general applicability, based on reparametrization of time, was used to provide counterexamples for two types of systems: phase coherent with funnellike geometry and non-phase-coherent with spirallike geometry. The same line of reasoning can be used for other oscillators to show the same point.

Based on recurrence plots, a measure of phase coherence was proposed (RTC index) that yields statistically significant results in discerning between noncoherent and phase-coherent behaviors in the tested systems. The main advantage of the RTC is that it does not depend on a phase variable, on the choice of an observable, or on the definition of a (Poincaré) section. The calculation is done only over a recurrence plot obtained from a time series.

ACKNOWLEDGMENTS

L.F. is grateful to Instituto Federal de Educação, Ciência e Tecnologia de Minas Gerais for an academic leave. Financial support from Coordenação de Aperfeiçoamento de Pessoal de Nível Superior (L.L.P., Grant No. 32001010015P8) and Conselho Nacional de Desenvolvimento Científico e Tecnológico (L.A.B.T., Grant No. 309268/2017-6; L.A.A., Grant No. 302079/2011-4) is gratefully acknowledged.

[1] M. G. Rosenblum, A. S. Pikovsky, and J. Kurths, Phys. Rev. Lett. **76**, 1804 (1996).
[2] C. Stam, Clin. Neurophysiol. **116**, 2266 (2005).
[3] J. Oh, E. Reischmann, and J. A. Rial, Quat. Sci. Rev. **83**, 129 (2014).
[4] A. Groth and M. Ghil, Chaos **27**, 127002 (2017).
[5] L. Freitas, L. A. B. Torres, and L. A. Aguirre, Phys. Rev. E **97**, 052202 (2018).
[6] A. T. Winfree, *The Geometry of Biological Time* (Springer-Verlag, Berlin, 1980).
[7] S. Boccaletti, J. Kurths, G. Osipov, D. Valladares, and C. Zhou, Phys. Rep. **366**, 1 (2002).
[8] G. V. Osipov, B. Hu, C. Zhou, M. V. Ivanchenko, and J. Kurths, Phys. Rev. Lett. **91**, 024101 (2003).
[9] G. V. Osipov, J. Kurths, and C. Zhou, *Magnetic Phase Transitions*, Springer Series in Synergetics (Springer-Verlag, Berlin, 2007).
[10] D. V. Senthilkumar, M. Lakshmanan, and J. Kurths, Phys. Rev. E **74**, 035205(R) (2006).
[11] D. V. Senthilkumar, M. Lakshmanan, and J. Kurths, Chaos **18**, 023118 (2008).
[12] Y. Zou, R. V. Donner, and J. Kurths, Chaos **22**, 013115 (2012).
[13] Y. Zou, R. V. Donner, M. Wickramasinghe, I. Z. Kiss, M. Small, and J. Kurths, Chaos **22**, 033130 (2012).
[14] D. Farmer, J. Crutchfield, H. Froehling, N. Packard, and R. Shaw, Ann. NY Acad. Sci. **357**, 453 (1980).
[15] J. D. Farmer, Phys. Rev. Lett. **47**, 179 (1981).
[16] E. F. Stone, Phys. Lett. A **163**, 367 (1992).
[17] C. Letellier, P. Dutertre, and B. Maheu, Chaos **5**, 271 (1995).
[18] R. Gilmore, Rev. Mod. Phys. **70**, 1455 (1998).
[19] C. Letellier and R. Gilmore, *Topology and Dynamics of Chaos: In Celebration of Robert Gilmore's 70th Birthday*, World Scientific Series on Nonlinear Science Series A: Vol. 84 (World Scientific, Singapore, 2013).
[20] D. Pazó, I. P. Mariño, V. Pérez-Muñuzuri, and V. Pérez-Villar, Int. J. Bifurcation Chaos **10**, 2533 (2000).
[21] A. S. Pikovsky and J. Kurths, Phys. Rev. Lett. **78**, 775 (1997).
[22] C. S. Zhou, J. Kurths, E. Allaria, S. Boccaletti, R. Meucci, and F. T. Arecchi, Phys. Rev. E **67**, 066220 (2003).
[23] S. Boccaletti, E. Allaria, and R. Meucci, Phys. Rev. E **69**, 066211 (2004).
[24] J. T. C. Schwabedal, A. Pikovsky, B. Kralemann, and M. Rosenblum, Phys. Rev. E **85**, 026216 (2012).
[25] J.-P. Eckmann, S. O. Kamphorst, and D. Ruelle, Europhys. Lett. **4**, 973 (1987).
[26] M. C. Romano, M. Thiel, J. Kurths, I. Z. Kiss, and J. L. Hudson, Europhys. Lett. **71**, 466 (2005).
[27] L. A. Aguirre and C. Letellier, Phys. Rev. E **83**, 066209 (2011).
[28] G. F. Amaral and E. G. Nepomuceno, Chaos, Solitons & Fractals **109**, 31 (2018).
[29] C. Chicone, *Ordinary Differential Equations with Applications*, Texts in Applied Mathematics (Springer, New York, 2006).
[30] The Wilcoxon-Mann-Whitney U test was performed over all and over each of the 100 Monte Carlo runs and, in both cases, yields a p value $\ll 10^{-35}$.
[31] D. Li, Phys. Lett. A **372**, 387 (2008).